

# Convective shifts of iron lines in the spectrum of the solar photosphere

V.A. Sheminova and A. S. Gadun

Main Astronomical Observatory, National Academy of Sciences of Ukraine  
Zabolotnoho 27, 03689 Kyiv, Ukraine  
E-mail: shem@mao.kiev.ua

## Abstract

The influence of the convective structure of the solar photosphere on the shifts of spectral lines of iron was studied. Line profiles in the visible and infrared spectrum were synthesized with the use of 2-D time-dependent hydrodynamic solar model atmospheres. The dependence of line shifts on excitation potential, wavelength, and line strength was analyzed, along with the depression contribution functions. The line shifts were found to depend on the location of the line formation region in convective cells and the difference between the line depression contributions from granules and intergranular lanes. In visible spectrum the weak and moderate lines are formed deep in the photosphere. Their effective line formation region is located in the central parts of granules, which make the major contribution to the absorption of spatially unresolved lines. The cores of strong lines are formed in upper photospheric layers where is formed reversed granulation due to convection reversal and physical conditions change drastically there. As a consequence the depression contributions in the strong line from intergranular lanes with downflows substantially increase. This accounts for smaller blue shifts of strong lines. In infrared spectrum the observed decrease in the blue line shifts is explained by the fact that their effective line formation regions lie higher in the photosphere and extend much further into the reversed granulation region due to the opacity rise with the increase of line wavelength. Additionally the effective line formation depths of the synthesized visible and infrared Fe I lines and their dependence on line parameters is discussed.

## 1 Introduction

If the motion of the Sun-Earth system is taken into account as well as the correction for the gravitational red shift (636 m/s) caused by the difference between the gravitational potential of the solar atmosphere and the Earth is introduced, the most absorption lines observed at the center of the solar disk are shifted towards shorter wavelengths with respect to laboratory lines. The observed blueshifts of the solar iron lines are 300–400 m/s on the average [1, 3, 4, 5, 6, 27, 29, 33]. They were measured to an accuracy of 100 m/s in the range from 0 to 1 km/s. It is found that the blueshifts decrease with growing height of line formation as suggested by its dependence on excitation potential. The largest blueshifts are observed in weak lines with high excitation potentials, while the smallest blueshifts are in strong lines. The redshifts were found to be small in some strong lines in the visible spectrum, but they can be as large as 1 km/s in the ultraviolet lines in the range 195–200 nm [33]. Some “reddening” of blueshifts was also noted in active photospheric regions [3, 4]. The blueshifts observed in weak and moderate lines can be

explained by a decrease with height in the velocity of the convective motions along the line of sight towards the observer [5, 6]. The formation region of strong photospheric lines extends to the layers of reversed granulation, a pattern comparable to the granulation but with reversed brightness modulation. The matter at the center of convection cells becomes cooler than in descending intergranular lanes, but it still moves upwards. An inverse correlation between brightness and shifts was found in the cores of very strong lines in the visible and infrared spectrum [23]. The effects of convection overshoot in the solar photosphere [28] is believed to be the cause of the observed line redshifts.

The objective of this study is the effect of reversed granulation and the role of granules and intergranular lanes in the formation of spatially unresolved spectral lines and the cause of the “reddening” of blueshifts of strong lines. Such a study is possible today due to the remarkable progress in the simulation of solar granulation and its evolution [2, 7, 28, 31, 34] and in the development of the idea of depression contribution functions [20, 21, 24, 26]. Based on 2-D hydrodynamic model atmospheres [19], we synthesized Fe I lines and calculated their shifts. We used contribution functions to investigate the region of line formation in convection cells and to analyze the influence of physical conditions in the granular photosphere on the shifts of the synthesized lines.

## 2 Hydrodynamic model of solar granulation

The sequence of single-scale (one-cell) and multi-scale two-dimensional nonstationary hydrodynamic (HD) models of solar granulation built by Gadun [8, 19] were used more than once for the synthesis of photospheric lines [9, 10, 11, 12, 13, 14, 16, 17, 18]. Such sequence models proved to be capable of reproducing satisfactorily the manifestations of convective motions, the asymmetry and shifts of lines in particular. Comparison of the profiles synthesized with the use of 3-D and 2-D HD models [8] showed that the single-scale 2-D models are inferior to 3-D models in reproducing the observed line asymmetry because their inhomogeneity spectrum is narrower. Nevertheless, the use of 2-D models [19] for the synthesis of spectral lines is justified when we want to obtain the overall picture of the processes in the superadiabatic regions in the photospheres of the Sun and solar-like stars.

The 2-D HD model sequence we used in our study treats the radiative transfer on the basis of the monochromatic absorption coefficient depending on frequency, and the atomic and molecular line absorption is taken into account through the use of the opacity distribution function (ODF) method [25]. The thermal convection in the solar envelope was assumed to be quasi-stationary with a single convective flow in the simulation region, and this flow represented the only granulation scale. In building the HD models we assumed that convective flows were quasi-stationary in time, the horizontal size of convective cells did not change in the course of their evolution, and convective cylinders always extended downwards as deep as permitted by the simulation region (1100 km below the surface level in the models). These models were called the steady-stable (SS) models by their author. The dimensions of the calculated region were 1400 km in the horizontal direction and 1960 km in the vertical direction (the atmospheric layers extended to 800 km). The spatial step was 28 km. The total duration of simulation was 50 min of the real solar time with a time step of 30 s between the models. Test calculations showed that such a duration was sufficient for a correct representation of five-minute oscillations in the spectral line calculations. This time-dependent sequence of 2-D models for the solar disk center includes 100 models (or 100 snapshots) consisting of 48 columns. Each column is located along the line of sight. A more detailed description of 2-D HD models of this type can be found in [9, 19].

### 3 Spectral line synthesis

To find the dependence of line shifts on principal line parameters, we used certain artificial Fe I lines. The central line depths ( $d$ ), lower excitation potentials ( $EP$ ), and wavelengths of the artificial lines was specified in a wide range of actual Fe I line parameters. Then the product of abundance and oscillator strength  $Agf$  was chosen for every line in accordance with its central depth. The lines were synthesized in the 1.5-D LTE solution of the transfer equation [15] with the use of the SS-model sequence – this means that the line profiles were calculated for each column in all snapshots as for a plane-parallel atmosphere. Then the obtained line profiles were averaged over all columns in each snapshot and over all snapshots. The result was a line profile averaged over space and time.

The central wavelength of a synthetic profile  $\lambda$  was determined by fitting a fourth-degree polynomial to the profile core. The accuracy of the procedure was  $\pm 50$  m/s. The shift of the synthetic line with respect to the laboratory central wavelength  $\lambda_0$  was calculated, with allowance made for the gravitational shift, in radial velocity units by the formula  $V_R = c(\lambda - \lambda_0)/\lambda_0 - 2.12 \cdot 10^{-6}c$ ,  $c$  being the light velocity. Test calculations demonstrated that the shift of the averaged line profile synthesized with the full SS-model sequence (100 snapshots) differs insignificantly from the shift of the line profile calculated with a snapshot averaged over all 100 snapshots. This allowed us to substantially cut the calculations by using the averaged SS model only. For line shift analysis we used the calculated line profiles for each column in the averaged SS model and the profile averaged over all columns. We also used the depression contribution functions calculated for each profile point and the effective formation heights. These latter are calculated as the weighted mean for the depression contribution function [20, 21].

### 4 Analysis of calculation result for lines in the visible spectrum

The plots of line shifts of synthetic Fe I lines for various wavelengths, line strengths, and heights of formation (Fig. 1) suggest that these calculated shifts behave in the same fashion that the observed shifts [1, 3, 6]. Weak lines with high  $EP$  at shorter wavelengths have the largest blueshifts that correspond to the largest negative radial velocities. Strong lines, whose central parts are formed high in the photosphere, feature redshifts. The typical strong narrow lines with  $d = 0.8$ , equivalent width  $W = 8$  pm, and  $\lambda = 600$  nm show the largest redshifts (positive radial velocities). Our results also demonstrate a clear dependence of shifts on wavelength (Fig. 1a), although no such dependence was found in the observed line shifts [1]. It seems likely that the authors could not reveal this dependence because they ignored the differences in the central depths of the lines observed. In general, we confirm that the line blueshifts decrease with growing line wavelength, line strength, and effective height of line formation.

To understand the causes of formation line shifts, we considered the snapshot of the simulated convective cell (the averaged SS 2-D model) and the depression contribution functions ( $CF$ ) of synthetic Fe I lines with different line parameters on Fig. 2. The isotherms (dashed lines), which demonstrate the temperature distribution in the convective cell, show that the temperature inversion in the photospheric layers begins above 200 km. This is the region of the so-called reversed granulation caused by convective reversal. Here the isotherms, which are convex over the granule center, become concave. The velocity field marked by arrows illustrates the motions in the convective cell: vertical upflows in the central part and downflows at the cell periphery. The central region of convective cell will be call granule, and the regions with downflows will be call intergranular lanes, as adopted for the observed granulation structure in

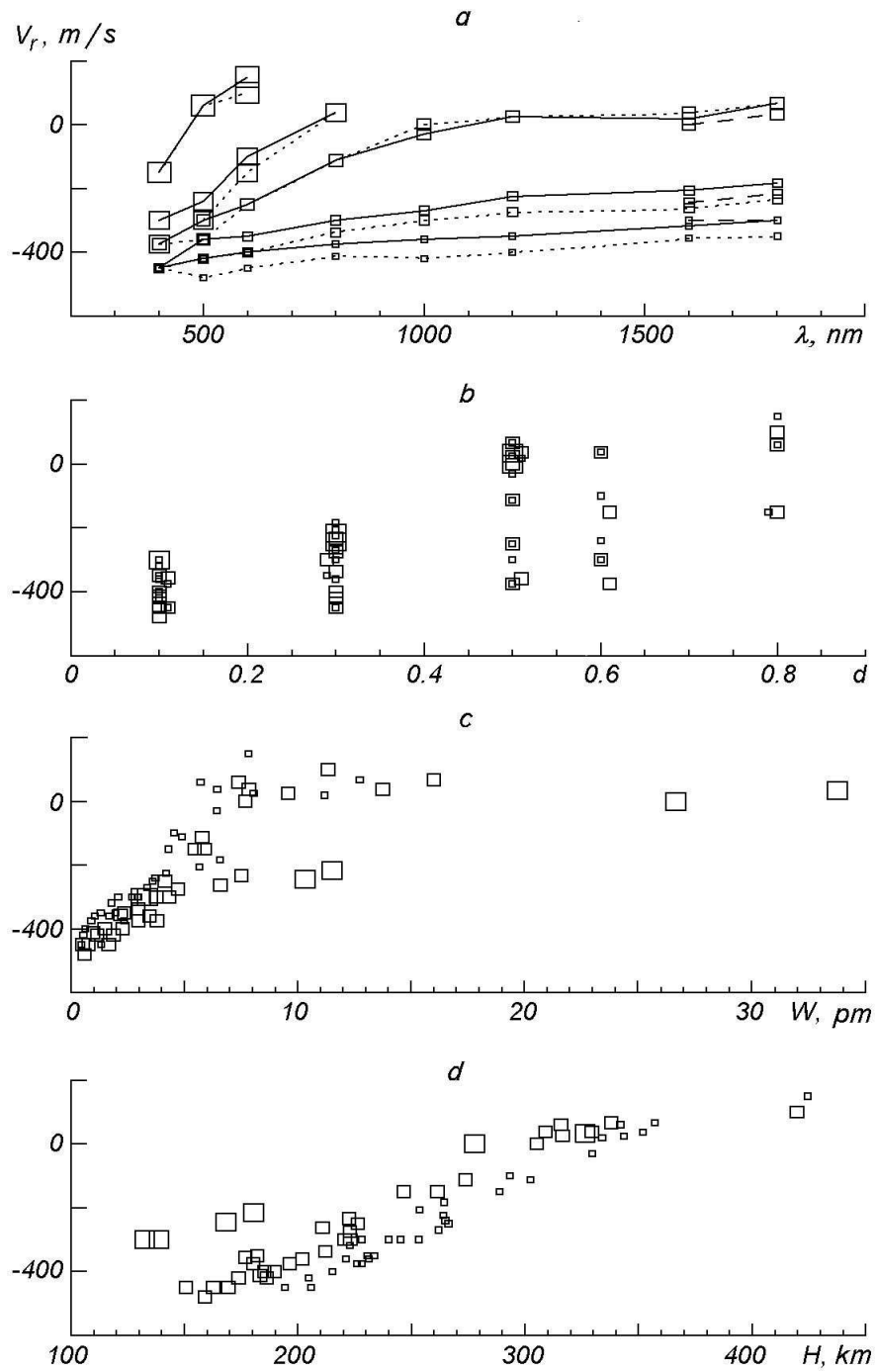


Figure 1: Dependence of convective shifts of synthesized Fe I lines on wavelength (a), central depth (b), equivalent width (c), and height of formation (d). Solid line:  $EP = 2.5$  eV, dotted line:  $EP = 4.25$  eV, dashed line:  $EP = 6.4$  eV. Size of the squares grows with line strength (a),  $d = 0.1, 0.3, 0.5, 0.6, 0.8$ , and excitation potential (b,c,d),  $EP = 2.5, 4.25, 6.4$  eV.

the photosphere. In addition, we also distinguish a region with predominantly horizontal flows of matter located between the granule and intergranular lanes. The depression contribution function contours calculated in each column for the core of synthesized line were plotted on the snapshot of the convective cell from the averaged SS 2-D model. The solid thick line is the contour corresponding  $0.5CF_{max}$ . It outlines the region of effective depression contributions. Inside this contour, there are the contour of the greatest contributions corresponding  $0.75CF_{max}$ , and outside it two contours corresponding  $0.25CF_{max}$  and  $0.1CF_{max}$  are plotted. Here  $CF_{max}$  is the maximum of contribution functions calculated in each model column for line core. Outside the outermost contour the line absorption is insignificant. Fig 2 shows the contours for the weak line (a) and strong line (b); for moderate line with  $EP = 2.5$  (c) and  $EP = 4.25$  (d). Figs 2e,f,g,h show the  $CF$  contours for moderately strong line depending on the wavelength. It is interesting that lines with wavelengths about  $\lambda$  800 nm are only partially formed in the granulation inversion zone, while the lines with  $\lambda$  1600–1800 nm are almost completely formed there. The depression contribution from intergranular lanes is greater for infrared lines. Figure 2h illustrates the appearance of new small effective contribution regions in intergranular lanes. In general, the depression contribution contours for different lines plotted on the background of a snapshot of a convection cell clearly demonstrated that intergranular lanes can play different part in the formation of absorption lines depending on line wavelength and central line depth.

Apart from contribution functions, we also considered the individual line profiles calculated for each column in the simulated convective cell. We selected the most typical line profiles formed in intergranular lanes, in region with predominantly horizontal motions, and in the central parts of the granule. Figure 3 displays these line profiles as well as the profiles of the line formation heights. It should be noted that the line formation height profiles are quite intricate for inhomogeneous photosphere models as different from the homogeneous models. In the latter case these height profiles are always completely symmetric. The synthetic line profiles at the center of granule are slightly asymmetric and have always blueshifts (kind I). The profiles in the regions with predominantly horizontal motions have weak asymmetry and are virtually not shifted (kind II). They differ insignificantly from kind I profiles in strength and width. The profiles in intergranular lanes are strongly asymmetric and have large redshifts (kind III). Their cores are weaker and they are markedly widened as compared to the profiles of kinds I and II. Depending on the line parameters the shape and shift of the profile of I, II, III kinds slightly change, but its major features remain the same. It should be noted that the line profiles observed in the spectra obtained with very high spatial and spectral resolution for bright, moderately bright, and dark regions of photospheric granulation [22] are in complete agreement with our synthetic profiles. This confirms to a degree the correctness of our calculations with the use of 2-D HD models.

Comparison of the profile averaged over the whole simulation region with the profiles of kinds I, II, and III (Fig. 3a) shows that the largest contribution to the averaged profile core of a weak line ( $d = 0.1$ ) comes from kind I and II profiles, i.e., from the whole granule and region with predominantly horizontal motions. The contribution of the kind III profiles to the average profile of the weak line is noticeable in the red wing of the line only — the wing is more extended, increasing the profile asymmetry in extended wings. The blue wing of the average profile of the weak line, as the line core, is formed in the main by kind I and II profiles. It is therefore concluded that the core shift and the shape of the blue wing of the weak line are controlled primarily by the ascending motions in the central parts of granules, while the shape of the red wing is also affected by the descending motions in intergranular lanes. From Fig. 3c we can estimate the effective heights of formation of the core and the wings in the averaged profile of a weak line ( $d = 0.1$ ). This is the layers in the range of 140–160 km for the core, 80–

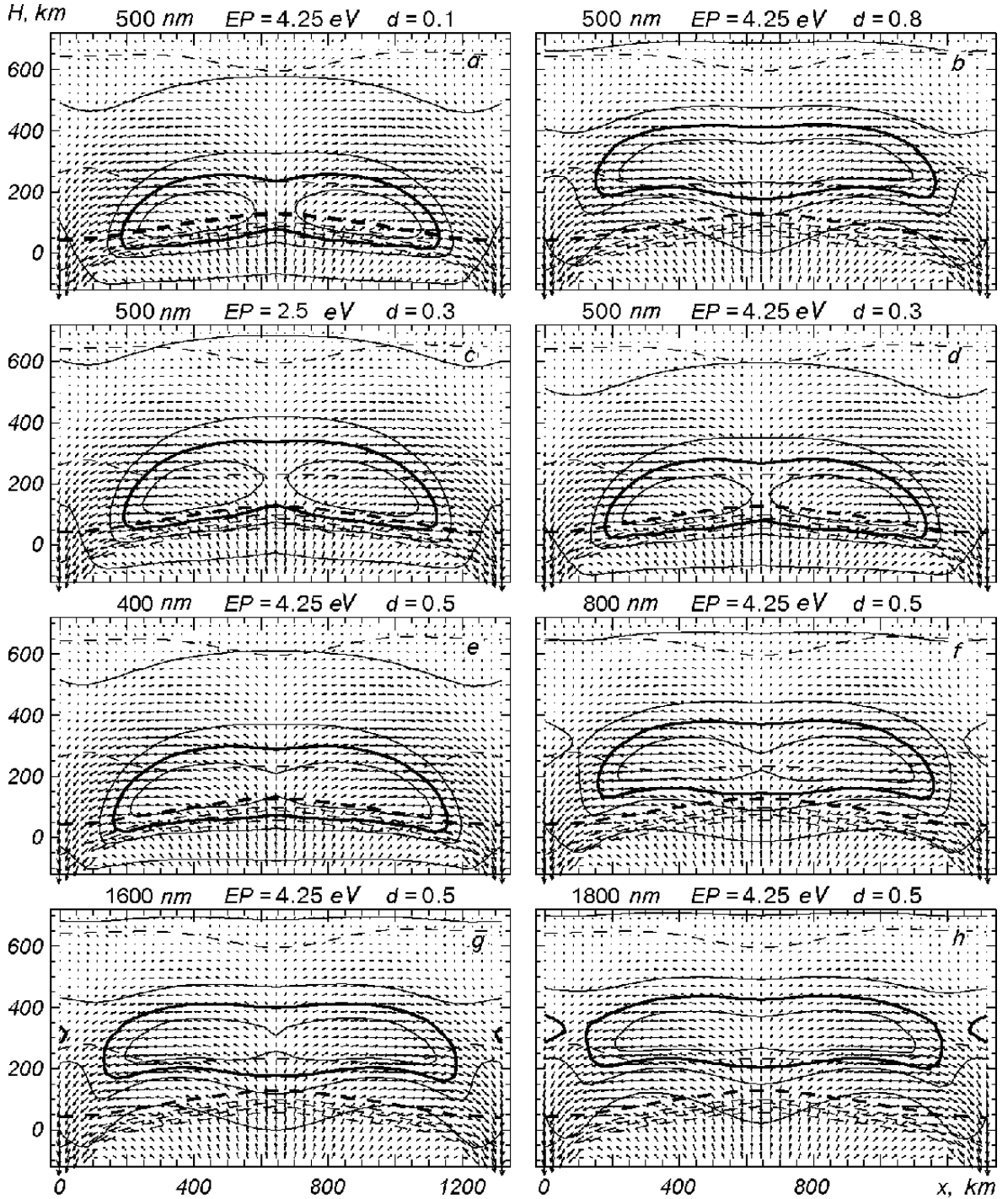


Figure 2: The snapshot of the convective cell from the averaged SS 2-D model and contours of depression contribution functions (solid line) for various synthesized Fe I lines: weak line and strong line (a,b); moderate line with low and high excitation potential (c,d); moderate line with different wavelengths (e,f,g,h). Thick solid line marks contour corresponding  $0.5CF_{max}$ . Dashed line: isotherms (4000, 4000, 6000, 7000, 8000, 9000, 10000 K from the top down), solid dashed line: surface level with the Rosseland optical depth equal to unity. Arrows indicate the velocity direction and their length is proportional to the velocity amplitude.

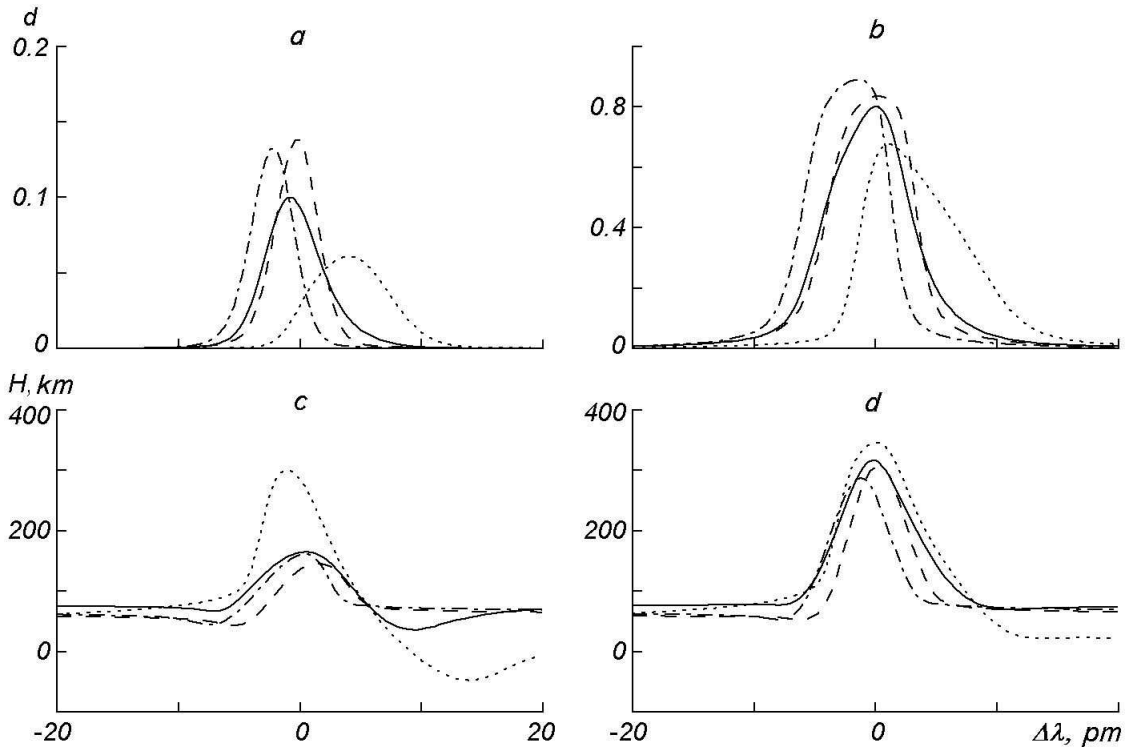


Figure 3: Three kinds of line profiles calculated in the simulated convection cell for a weak line (a) and a strong line (b) at  $\lambda = 500 \text{ nm}$ ,  $EP = 4.25 \text{ eV}$ . Dot-and-dash line: kind I profile from the central region, dashed line: kind II profile from the region with horizontal motions, dotted line: kind III profile from intergranular lanes; solid line: average profile. The profile of effective heights of line formation (c,d) are in response to changing line profiles (a,b).

140 km the blue wing, and 50–140 km for the red wing. The effective heights of the moderate line ( $d = 0.5$ ) is located 150 km higher than the above weak line. All other details relative to different kinds of profiles are similar. In the strong line ( $d = 0.8$ , Fig. 3b) the kind III profiles formed in intergranular lanes are much stronger, and the line asymmetry is stronger because of temperature drop in the upper granular layers. As a result, the shape of the unresolved profile of the strong line change, and the blueshift of the line core decreases. The strong line core is formed at heights of 280–350 km (Fig. 3d) in the reversed granulation region.

The above analysis of the shape and shifts of synthesized line profiles allows us to conclude that the red wing of spatially unresolved line may be regarded as an indicator of the role which intergranular lanes play in the formation of absorption lines. The more extended red wing as compared to the blue wing, the larger is the depression contribution in the spectral line from intergranular lanes. The shape of blue wings and shifts of weak and moderate lines in particular, depend completely on the physical conditions in the central parts of granules.

## 5 Analysis of infrared lines

Lists of numerous unblended infrared lines in three bands of the solar spectrum –  $J$  (1.00–1.34  $\mu\text{m}$ ),  $H$  (1.5–1.8  $\mu\text{m}$ ), and  $K$  (1.9–2.5  $\mu\text{m}$ ) – were published recently in [30, 32]. The H band lines are most frequently used in various spectral investigations of stellar atmospheres. These lines have some advantages over other infrared lines. The continuum opacity is at a minimum

in the  $H$  band, and we can see deeper photospheric layers in these lines as compared to the lines of  $J$  and  $K$  bands or the visible lines. For instance, the Fe I lines with very high excitation potentials and large Lande factors are very sensitive to the magnetic fields located at the photosphere base. It is also well known that the contrast of continuum intensity is smaller for infrared lines, and this allows us to suggest that they are not formed in granulation cells in the same way as the lines in the visible range. Some differences between the profiles of the infrared and visible lines with the same principal parameters are attributed to the strong wavelength dependence of absorption coefficient. The selective absorption grows proportionally to wavelength, while the continuous absorption depends to a great extent on the sort of absorbers. Recall that the continuum opacity in the infrared range attains its maximum at  $\lambda$  1000 nm, diminishes with increasing wavelength to a minimum at  $\lambda$  1600 nm which is approximately of the same magnitude as the minimum at  $\lambda$  400 nm, and then grows again. Generally, the total opacity is always greater in the infrared lines than in the lines of the visible spectrum due to the increase of the selective absorption coefficient. As a result, the regions of formation of any infrared lines are located in higher layers and are more extended into intergranular lanes. These effects increase with line strength and excitation potential. The excitation potentials for the infrared Fe I lines range from 2 to 6.4 eV, and for a line with  $d = 0.5$ ,  $\lambda = 1800$  nm, and  $EP = 4.25$  eV, for instance, the region of its core formation is located completely in the reversed granulation layers. In intergranular lanes the line formation region shifts higher (Fig. 2h) with respect to the visible lines of the same line strength (Fig. 2e). The depression contribution from intergranular lanes in the core of a visible line is about 25 percent of the maximum contribution, while for infrared lines it is 50 percent and more.

The depression contributions of intergranular lanes to the infrared line affects the shape of average line profiles. Figure 4 shows line profiles with a central line depth of 0.5 and wavelengths of 400, 800, 1600, and 1800 nm as well as their formation height profiles. All infrared line profiles are nearly twice as wide as the profiles of similar visible lines. The widest and the most asymmetric profile is formed in intergranular lanes, where the temperature and velocity gradients are large, and as a result the asymmetry in the red wings of average profiles is greater than in the visible lines. The effective height profiles also suggest that the formation regions of infrared lines are more extended in height. Weak lines are formed in the range from  $-100$  km to 300 km, while strong lines are formed at heights from 100 km to 330 km.

Fig. 5 shows the effective heights of formation of Fe I lines in the infrared and visible spectrum. It should be noted that the weak iron lines ( $d < 0.1$ ,  $\lambda\lambda$  1600–1800 nm,  $EP = 6.4$  eV) are formed in the deepest photospheric layers. The blueshifts of these deepest-formed infrared lines are not the largest ones (see Fig 1a) due to the effect of additional absorption from the lanes. Therefore the blueshifts of infrared weakest lines are smaller than the blueshifts of the visible weakest lines with  $EP = 4.25$  eV.

Thus, the infrared iron lines are mainly formed in the reversed granulation zone. Therefore intergranular lanes play considerable importance role in the formation of the cores of infrared lines. This accounts for the observed decrease of blueshifts of infrared spectrum as compared with the visible spectrum.

## 6 Conclusion

We synthesized the Fe I lines in the framework of the 2-D HD models of solar granulation and determined the wavelength shifts of these lines and their dependence on the line parameters. The derived relations fit quite well the observation data. Additionally we calculated the depression contribution functions to demonstrate that the line shifts are determined by the location



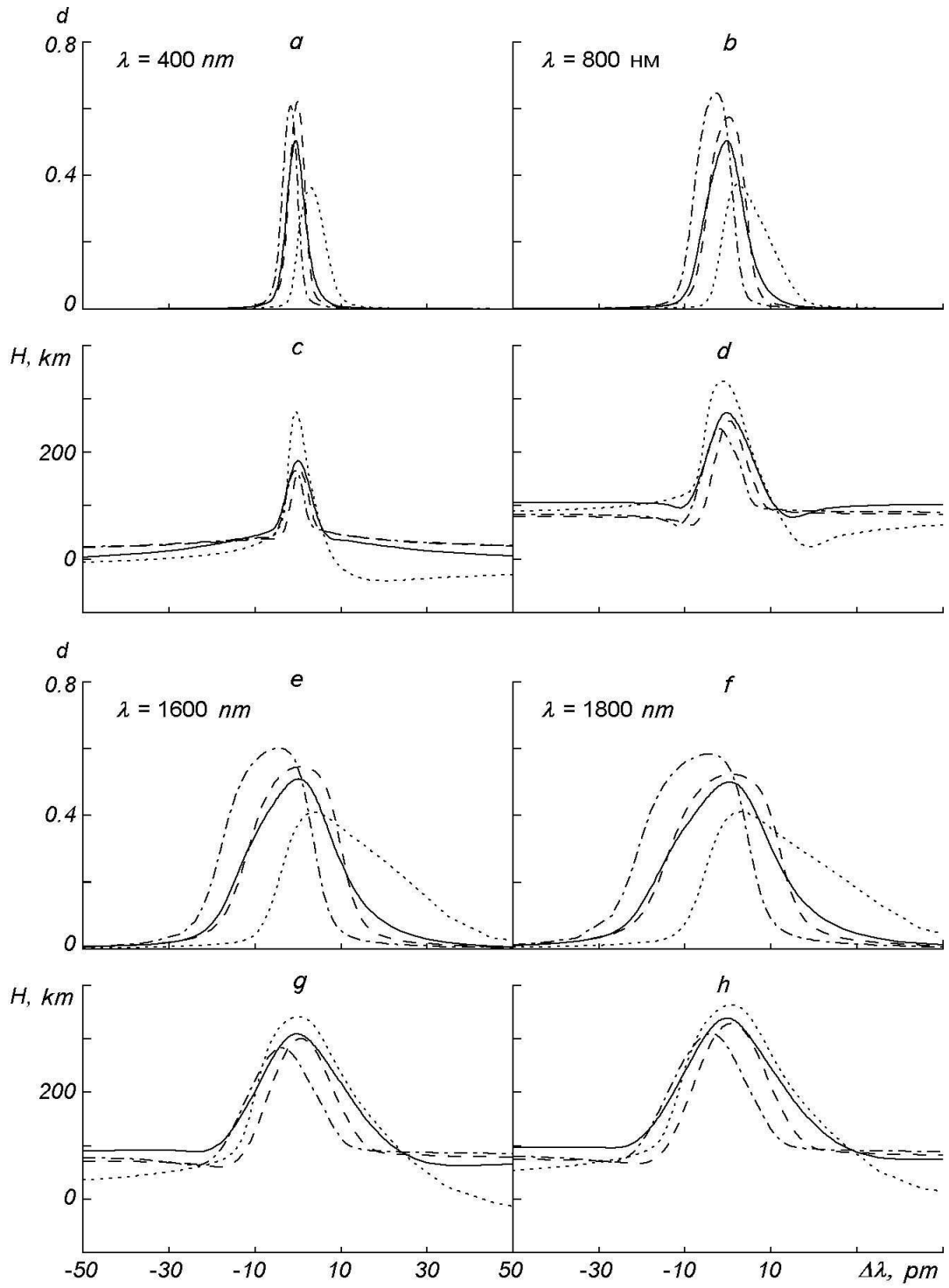


Figure 4: The same as in Fig. 3, but for moderate lines with  $d = 0.5$ ,  $EP = 4.25$  eV, and  $\lambda 400$  (a),  $\lambda 800$  (b),  $\lambda 1600$  (e),  $\lambda 1800$  nm (f).

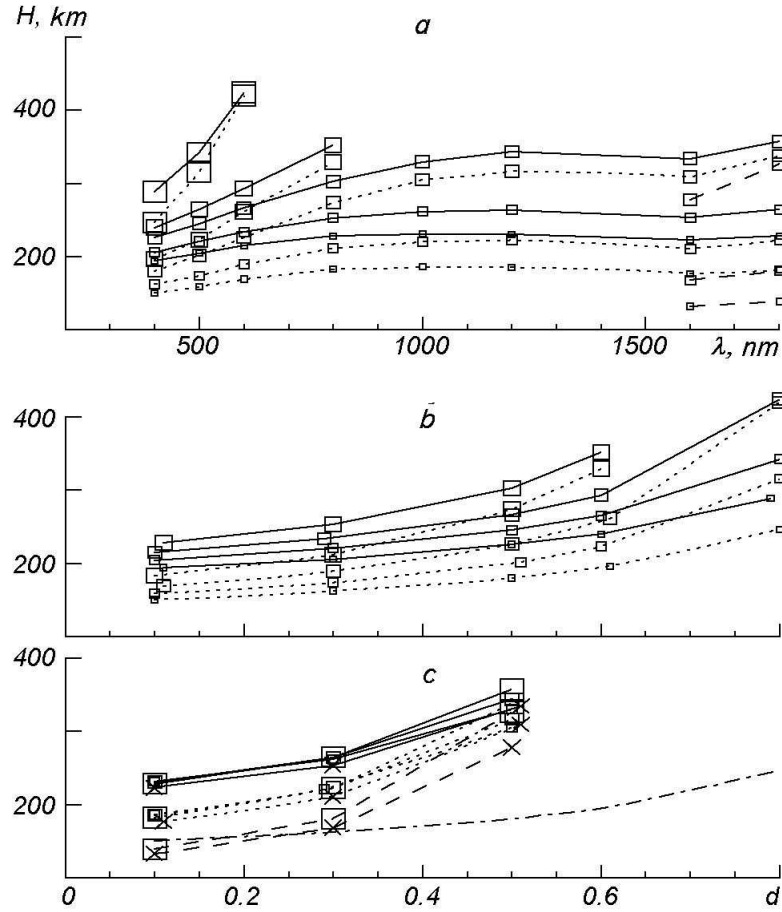


Figure 5: Effective heights of formation for artificial synthesized Fe I lines depending on wavelength (a) and central depth for the visible (b) and infrared (c) spectrum. Solid line:  $EP = 2.5$  eV, dotted line:  $EP = 4.25$  eV, dashed line:  $EP = 6.4$  eV. Size of the squares grows with line strength  $d = 0.1, 0.3, 0.5, 0.6, 0.8$  (a), and wavelength  $\lambda = 300, 400, 500, 600, 800$  nm (b) and  $\lambda = 1000, 1200, 1800$  nm (c). Crosses mark  $\lambda = 1600$  nm. Dot-and-dash line marks  $\lambda = 400$  nm,  $EP = 4.25$  eV shown for comparison.

of effective line formation region in convection cells. Obtained results confirmed the convective character of the line shifts.

Analysis of the line profiles and the corresponding contribution functions showed that the contribution from granules and intergranular lanes to the depression of spatially unresolved spectral lines is essentially different for weak and strong lines as well as for lines in the visible and infrared ranges. In the visible range weak and moderate lines originate deep in the photosphere, where the classical convection structure is not disrupted, i.e., hot masses move upwards and cool masses descend. Cores of strong iron lines are formed in the upper photosphere, in the convection reversal zone, where occurs a temperature inversion as well as granulation inversion. The temperature in the ascending central regions of a convection cell is lower than in descending regions. The temperature inversion increases the role of intergranular lanes in the formation of the depression of the spatially averaged line. As a result, the depression contribution from the regions with downflows grows, and the line blueshifts diminish to zero or even become red. In the infrared spectrum the effect of reserved granulation on the line formation is stronger. Due to growth of line opacity with wavelength the level of effective line formation is shifted higher into the photosphere where are manifested the reserved granulation zone. Therefore the line blueshifts in the infrared spectrum are smaller than in the visible spectrum.

Convective motions cause the asymmetry of spectral line profiles. The blue wings and cores of spectral lines are mainly formed in the central parts of granules, where upflows prevail. The red wings are mainly formed in intergranular lanes with downflows. Greater contributions from intergranular lanes in the depression of strong lines results in the strengthening of red wings of absorption lines and consequently a greater asymmetry, as compared to weak and moderate lines. Therefore the red wing of a spectral line can be regarded as an indicator of the additional absorption in intergranular lanes.

We have found that the weak infrared Fe I lines with  $\lambda \approx 1600$  nm and very high excitation potentials (about 6.4 eV) are formed at the deepest photospheric layers. Such lines may be of prime importance in diagnostics of stellar atmospheres.

## References

- [1] C. Allende Prieto, R. J. Garcia Lopez, “Fe I line shifts in the optical spectrum of the Sun,” *Astron. and Astrophys. Suppl. Ser.*, vol. 129, no. 1, pp. 41–44, 1998.
- [2] I. N. Atroshchenko, A. S. Gadun, “Three-dimensional hydrodynamic models of solar granulation and their application to a spectral analysis problem,” *Astron. and Astrophys.*, vol. 291, no. 2, pp. 635–656, 1994.
- [3] P. N. Brandt, A. S. Gadun, V. A. Sheminova, “Absolute shifts of Fe I and Fe II lines in solar active regions (disk center),” *Kinematika i Fizika Nebes. Tel [Kinematics and Physics of Celestial Bodies]*, vol. 13, no. 5, pp. 75–86, 1997.
- [4] F. Cavallini, G. Ceppatelli, A. Righini, “Profile variations of some photospheric lines as observed in active regions across the solar disk,” *Astron. and Astrophys.*, vol. 205, no. 1/2, pp. 278–288, 1988.
- [5] D. Dravins, B. Larsson, Å. Nordlund, “Solar Fe II line asymmetries and wavelength shifts,” *Astron. and Astrophys.*, vol. 158, no. 1/2, pp. 83–88, 1986.

- [6] D. Dravins, L. N. Lindegren, Å. Nordlund, “Solar granulation: influence of convection on spectral line asymmetries and wavelength shifts,” *Astron. and Astrophys.*, vol. 96, no. 1/2, pp. 345–364, 1981.
- [7] B. Freytag, H. G. Ludwig, M. Steffen, “Hydrodynamical models of stellar convection. The role of overshoot in DA white dwarfs, A type stars, and the Sun,” *Astron. and Astrophys.*, vol. 313, no. 2, pp. 497–517, 1996.
- [8] A. S. Gadun, “Multidimensional hydrodynamic models of the solar atmosphere: effects of radiative transfer in a multidimensional perturbed medium,” *Kinematika i Fizika Nebes. Tel [Kinematics and Physics of Celestial Bodies]*, vol. 11, no. 3, pp. 54–72, 1995.
- [9] A. S. Gadun, “Iron abundance derived from two-dimensional inhomogeneous solar model atmosphere. Fe I and Fe II lines (center of the disk),” *Kinematika i Fizika Nebes. Tel [Kinematics and Physics of Celestial Bodies]*, vol. 12, no. 4, pp. 19–31, 1996.
- [10] A. S. Gadun, “Spatial variations in the Li I  $\lambda$  671 nm resonance line in two-dimensional simulated granulation,” *Kinematika i Fizika Nebes. Tel [Kinematics and Physics of Celestial Bodies]*, vol. 15, no. 2, pp. 153–159, 1999.
- [11] A. S. Gadun, A. Hanslmeier, “Variations of line parameters and bisectors over granular-intergranular regions in the 2-D artificial solar granulation,” *Kinematika i Fizika Nebes. Tel [Kinematics and Physics of Celestial Bodies]*, vol. 13, no. 3, pp. 24–48, 1997.
- [12] A. S. Gadun, A. Hanslmeier, “Correlation analysis of two-dimensional solar atmosphere,” *Kinematika i Fizika Nebes. Tel [Kinematics and Physics of Celestial Bodies]*, vol. 16, no. 2, pp. 121–129, 2000.
- [13] A. S. Gadun, A. Hanslmeier, “Fe II lines in the problem of the diagnostic of solar photospheric shocks,” *Kinematika i Fizika Nebes. Tel [Kinematics and Physics of Celestial Bodies]*, vol. 16, no.2, pp. 130–137, 2000.
- [14] A. S. Gadun, Ya. V. Pavlenko, “1-D and 2-D model atmospheres iron and lithium LTE abundances in the Sun,” *Astron. and Astrophys.*, vol. 324, no. 1, pp. 281–288, 1997.
- [15] A. S. Gadun, V. A. Sheminova. SPANSAT: Program for Calculating the LTE Absorption Line Profiles in Stellar Atmospheres, Kyiv, 1988, Inst. Theor. Phys., Academy of Sciences of UkrSSR, Preprint No. ITF-88-87P.
- [16] A. S. Gadun, Yu. Yu. Vorob’ev, “Parameters of artificial granules in two-dimensional hydrodynamic numerical simulation of solar granulation,” *Astron. Zhurn.*, vol. 73, no. 4, pp. 623–632, 1996.
- [17] A. S. Gadun, A. Hanslmeier, K. N. Pikalov, “Bisectors and line-parameter variations over granular and intergranular regions in 2D artificial granulation,” *Astron. and Astrophys.*, vol. 320, no. 3, pp. 1001–1012, 1999.
- [18] A. S. Gadun, S. K. Solanki, A. Johannesson, “Granulation near the solar limb: observations and 2-D modeling,” in: *Motions in the Solar Atmosphere*, pp. 201–204, Kluwer, Dordrecht, 1999.
- [19] A. S. Gadun, S. K. Solanki, S. R. O. Ploner, et al., *Scale-Dependent Properties of 2-D Artificial Solar Granulation*, Kiev, 1998. National Academy of Sciences of Ukraine, Main Astronomical Observatory Preprint (MAO-98-4E).

- [20] U. Grossman-Doerth, “Height formation of solar photospheric spectral lines,” *Astron. and Astrophys.*, vol. 285, no. 3, pp. 1012–1018, 1994.
- [21] E. A. Gurtovrnko, V. A. Sheminova, A. P. Sarychev, “What is the difference between “emission“ and “depression“ contribution functions?” *Solar Phys.*, vol. 136, no. 2, pp. 239–250, 1991.
- [22] D. Kiselman, “High-spectral resolution solar observations of spectral lines used for abundance analysis,” *Astron. and Astrophys. Suppl. Ser.*, vol. 104, no. 1, pp. 23–77, 1994.
- [23] D. Kiselman, Å. Nordlund, “3D non-LTE line formation in the solar photosphere and the solar oxygen line abundance,” *Astron. and Astrophys.*, vol. 302, no. 2, pp. 578–586, 1995.
- [24] A. Kucera, H. Balthasar, J. Rybak, H. Wohl, “Heights of formation of Fe I photospheric lines,” *Astron. and Astrophys.*, vol. 332, no. 3, pp. 1069–1074, 1998.
- [25] R. L. Kurucz, *Opacities for Stellar Atmospheres (CD ROM 2)* 1993.
- [26] P. Magain, “Contribution function and the depths of formation of spectral lines,” *Astron. and Astrophys.*, vol. 163, no. 1/2, pp. 135–139, 1986.
- [27] D. Nadeau, J. P. Mailard, “Observational evidence of line shifts induced by the convective overshoot in the atmospheres of red giants,” *Astrophys. J.*, vol. 327, no. 1, pp. 321–327, 1988.
- [28] Å. Nordlund, D. Dravins, “Solar granulation. III. Hydrodynamic model atmospheres,” *Astron. and Astrophys.*, vol. 228, no. 1, pp. 155–183, 1990.
- [29] K. Pushmann, A. Hanslmeier, S. Solanki, *Solar and Stellar Granulations: IAU Symp. 178*, K. G. Strassmeier (Editor), p. 117, Vienna, 1995.
- [30] J. Ramsauer, S. K. Solanki, E. Biemont, “Interesting lines in infrared solar spectrum. II. Unblended lines between  $\lambda$  1.0 and  $\lambda$  1.8  $\mu\text{m}$ ,” *Astron. and Astrophys. Suppl. Ser.*, vol. 113, no. 1, pp. 71–89, 1995.
- [31] M. P. Rast, Å. Nordlund, R. F. Stein, J. Toomre, “Ionization effects in three-dimensional solar granulation simulations,” *Astrophys. J.*, vol. 408, no. 1, pp. L53–L56.
- [32] I. Ruedi, S. K. Solanki, W. Livingston, J. Harvey, “Interesting lines in infrared solar spectrum. III. A polarimetric survey between 1.5 and 2.50  $\mu\text{m}$ ,” *Astron. and Astrophys. Suppl. Ser.*, vol. 113, no. 1, pp. 91–106, 1995.
- [33] D. Samain, “In the ultraviolet spectrum of the quiet Sun redshifted?,” *Astron. and Astrophys.*, vol. 244, no. 1, pp. 217–227, 1991.
- [34] R. F. Stein, Å. Nordlund, “Simulations of solar granulation. I. General properties,” *Astrophys. J.*, vol. 499, no. 2, pp. 914–933, 1998.